

Sensitive dependence of network dynamics on network structure

Takashi Nishikawa,^{1,2} Jie Sun,^{3,4,5} and Adilson E. Motter^{1,2}

¹*Department of Physics and Astronomy, Northwestern University, Evanston, IL 60208, USA*

²*Northwestern Institute on Complex Systems, Northwestern University, Evanston, IL 60208, USA*

³*Department of Mathematics, Clarkson University, Potsdam, NY 13699, USA*

⁴*Department of Physics, Clarkson University, Potsdam, NY 13699, USA*

⁵*Department of Computer Science, Clarkson University, Potsdam, NY 13699, USA*

(Dated: January 20, 2024)

The relation between network structure and dynamics is determinant for the behavior of complex systems in numerous domains. An important longstanding problem concerns the properties of the networks that optimize the dynamics with respect to a given performance measure. Here we show that such optimization can lead to *sensitive dependence* of the dynamics on the structure of the network. Specifically, we demonstrate that the stability of the dynamical state, as determined by the maximum Lyapunov exponent, can exhibit a cusp-like dependence on the number of nodes and links as well as on the size of perturbations applied to the network structure. As mechanisms underlying this sensitivity, we identify discontinuous transitions occurring in the complement of optimal networks and the prevalence of eigenvector degeneracy in these networks. These findings establish a unified characterization of networks optimized for dynamical stability in diffusively coupled systems, which we illustrate using Turing instability in activator-inhibitor systems, synchronization in power-grid networks, and several other examples. Our results suggest that the network structure of a complex system operating near an optimum can potentially be fine-tuned for a significantly enhanced stability compared to what one might expect from simple extrapolation. On the other hand, they also suggest constraints on how close to the optimum the system can be in practice. Finally, the results have potential implications for biophysical networks, which have evolved under the competing pressures of optimizing fitness while remaining robust against perturbations.

I. INTRODUCTION

Building on the classical fields of graph theory, statistical physics, and nonlinear dynamics, as well as leveraging the recent advances in collecting large-scale network data, the field of network dynamics has flourished over the last 15 years. Much of the current effort in this area is driven by the premise that understanding the structure, the function, and the relation between the two will help explain the workings of natural systems and facilitate the design of engineered systems with expanded capability, optimized performance, and enhanced robustness [1]. There have been extensive studies on this structure-dynamics relation [2–4] in the context of network synchronization [5–15], reaction and/or diffusion dynamics [16, 17], as well as other types of dynamical processes on networks [18–23]. Many of these studies have led to systematic methods for enhancing the dynamics through network-structural modifications. Examples include controlling synchronization patterns of oscillators [24] or target wave patterns of excitable elements [25], suppressing epidemic spreading [26, 27], and enhancing the stability of synchronous oscillations [28–31]. The latter can be achieved by adjusting coupling strengths, removing nodes, rewiring links, and even removing links and adding nodes, and has been demonstrated in applications, with examples including systems of space-filling bearings [32] and coupled laser networks [33, 34].

A fundamental question at the core of the structure-dynamics relation is that of optimization: what network structure optimizes the dynamics of the system for a given function and what are the properties of such a network? The significance of addressing this question is two fold. First, knowledge on the properties of optimized structures informs sys-

tem architecture design. In power-grid networks, for example, the structures that maximize the stability of synchronous operation of power generators—a required condition for power grids to operate—could potentially be used to devise effective strategies for upgrading the system [35]. Second, the identification of the network structures that guarantee the best fitness of natural complex systems can provide insights into the mechanisms underlying their evolution. Examples of such systems include neuronal networks, whose synaptic connectivity structure is believed to have been optimized through evolution or learning for categorization tasks [36], synchronization efficiency [37], dynamical complexity [38, 39], information transfer efficiency [39, 40], and/or wiring cost [37]. The question of optimizing the network structure can be conceptualized as the problem of maximizing/minimizing a measure of dynamical stability, robustness, or performance over all possible configurations of links connecting the dynamical units.

Here we demonstrate that optimized dynamics is often highly sensitive to perturbations applied to the structure of the network. For concreteness, we focus on optimizing the stability against small changes in the network’s dynamical states, among all networks with a given number of nodes and links. We consider dynamical states in which the (time-dependent) states of the individual nodes are identical across the network, such as the states of agreement in consensus dynamics, states of synchronized periodic or chaotic oscillations, and states of equilibrium in diffusion processes. The appearance of sensitivity to structural perturbations generally depends on the class of networks and the nature of perturbations considered (Fig. 1), and here we establish the following two types of sensitivity:

	Directed networks	Undirected networks
Generic perturbations - Random link weight changes - Infinitesimal perturbation size - Finite network size	Sensitive for degenerate networks (more often for optimal networks) <i>arbitrary weights allowed</i>	Not sensitive ³ for any network <i>arbitrary weights allowed</i>
Non-generic perturbations - Changes in link density ¹ - Within set of optimal networks - In large-network limit	Not sensitive for any network (within the class of optimal networks) [0,1] or binary weights allowed ²	Sensitive ⁴ for UCM networks (within the class of MCC networks ⁵) [0,1] or binary weights allowed

FIG. 1. Sensitivity of dynamics on network structure. The stability of network dynamics can be sensitive to generic structural perturbations for directed networks and to optimized (and thus non-generic) structural perturbations for undirected networks. Footnotes: ¹In the finite-size case, the same results apply for changes in the number of nodes. ²In this case we are also able to show that the same result holds for networks with any integer-valued weights. ³Undirected networks are not sensitive to any link weight changes (not just to generic ones). ^{3,4}The two seemingly conflicting cases are consistent with each other (see Sec. IV B). ⁵MCC networks are locally optimal in the sense that the stability cannot be increased by rewiring a single link.

1. *Sensitivity of undirected networks to changing the number of nodes and links within the class of networks with optimized structure* (lower right red box in Fig. 1). This class consists of those networks characterized as having the Minimum possible size of the largest Components in their Complement (MCC) among all networks with the same number of nodes and links. We provide a full analytical characterization of the MCC networks of arbitrary finite size and study their behavior as the network size approaches infinity. For many combinations of the number of nodes and links, an MCC network actually satisfies a stronger condition, under which node groups of *equal* sizes are fully connected to each other, but have no internal links. Such networks are referred to as *uniform complete multipartite* (UCM) networks, and here we show that the UCM networks are optimal.
2. *Sensitivity of optimal directed networks to generic structural perturbations, i.e., small random changes to the link weights* (upper left red box in Fig. 1). We show that the tendency of optimization to induce spectral degeneracy underlies this sensitivity, which we expect to observe in many applications because spectral degeneracy appears to be common in real networks [41]. We also show that, even when the network has only approximate degeneracy (and thus approximate optimality), it exhibits the same sensitivity, at least approximately.

In addition to these two cases of sensitivity, we have results on the absence of sensitivity in the other two cases (blue boxes in Fig. 1). For networks under non-generic structural perturbations (bottom row in Fig. 1), our results provide a basis for a comprehensive theory of their spectral sensitivity/non-sensitivity. For networks under generic structural perturbations (top row in Fig. 1), we have a unified theory that determines the scaling of their spectrum with respect to the size of perturbations.

We illustrate the implications of our results using a general class of diffusively coupled systems for which we establish that their network spectrum determines the stability and other aspects of the dynamics to be optimized. Specific cases we

analyze include the rate of diffusion over networks, the critical threshold for Turing instability in networks of activator-inhibitor systems, and the synchronization stability in power grids and in networks of chaotic oscillators.

II. CLASS OF SYSTEMS CONSIDERED

We aim to address a wide range of network dynamics in a unified way. For this purpose we consider the dynamics of a network of coupled dynamical units governed by the following general equation with pairwise interactions:

$$\dot{\mathbf{x}}_i = \mathbf{F}(\mathbf{x}_i, \mathbf{H}_{i1}(\mathbf{x}_i, \mathbf{x}_1), \dots, \mathbf{H}_{in}(\mathbf{x}_i, \mathbf{x}_n)) \quad (1)$$

for $i = 1, \dots, n$, where n is the number of dynamical units (nodes), $\mathbf{x}_i = \mathbf{x}_i(t)$ is the column vector of state variables for the i -th unit at time t , and $\dot{\mathbf{x}}_i$ denotes the time derivative of \mathbf{x}_i . The function $\mathbf{F}(\mathbf{x}, \mathbf{y}_1, \dots, \mathbf{y}_n)$ is generally nonlinear and describes how the dynamics of unit i is influenced by the other units through intermediate variables $\mathbf{y}_j = \mathbf{H}_{ij}(\mathbf{x}_i, \mathbf{x}_j)$, where $\mathbf{y}_j = \mathbf{0}$ indicates no interaction. This means that the dynamics of an isolated unit is described by $\dot{\mathbf{x}} = \mathbf{F}(\mathbf{x}, \mathbf{0}, \dots, \mathbf{0})$. We assume that the dependence of \mathbf{F} on \mathbf{y}_j is the same for all j (or more precisely, that \mathbf{F} is invariant under any permutation of $\mathbf{y}_1, \dots, \mathbf{y}_n$). Thus, the topology of the interaction network and the strength of individual pairwise coupling are not encoded in \mathbf{F} , but rather in the (i, j) -dependence of the coupling function \mathbf{H}_{ij} . This extends the framework introduced in Ref. [42] and can describe a wide range of dynamical processes on networks, including consensus protocol [43, 44], diffusion over networks, emergence of Turing patterns in networked activator-inhibitor systems [45], relaxation in certain fluid networks [46], and synchronization of power generators [47] as well as other coupled identical and non-identical oscillators [42, 48–50].

For the class of systems described by Eq. (1), we consider *network-homogeneous states* given by $\mathbf{x}_1(t) = \dots = \mathbf{x}_n(t) = \mathbf{x}^*(t)$, where \mathbf{x}^* satisfies the equation for an isolated unit, $\dot{\mathbf{x}}^* = \mathbf{F}(\mathbf{x}^*, \mathbf{0}, \dots, \mathbf{0})$. Each of the example systems mentioned above exhibits such a state: uniform agree-

ment in consensus protocols, a synchronous dynamics in oscillator networks, uniform occupancy in network diffusion, uniform concentration in coupled activator-inhibitor systems, and the equilibrium in fluid networks. Note that certain non-homogeneous states can also be represented by such a solution by changing the frame of reference.

To facilitate the stability analysis, we make two general assumptions on the nature of node-to-node interactions when the system is close to the network-homogeneous state: (A-1) The interactions are “diffusive,” in the sense that the coupling strength between two nodes, $\mathbf{H}_{ij}(\mathbf{u}, \mathbf{v})$, is to first order proportional to the difference between their states, $\mathbf{v} - \mathbf{u}$. In particular we assume that the coupling strength vanishes as the node states become equal. (A-2) There is a constant coupling matrix $A = (A_{ij})$ encoding the structure of the network of interactions, in the sense that the proportionality coefficient (the “diffusion constant”) in assumption (A-1) can be written as $A_{ij} \cdot \mathbf{G}(t)$, where the scalar A_{ij} represents the strength of coupling from node j to node i , and the vector-valued function $\mathbf{G}(t)$ is independent of i and j . Under these assumptions, we define a stability function $\Lambda(\alpha)$ for each complex-valued parameter α (see Appendix A), which captures the factors determining the stability of the network-homogeneous state but is independent of the network structure. This function, referred to as a master stability function in the literature, was originally derived for a general class of systems that is different from the one we consider here [42, 49]. The influence of the network structure on the stability is only through the (possibly complex) eigenvalues of the Laplacian matrix L , defined by

$$L_{ij} := d_i \delta_{ij} - A_{ij}, \quad d_i := \sum_{j=1}^n A_{ij}. \quad (2)$$

Note that L always has a null eigenvalue $\lambda_1 = 0$ associated with the eigenvector $(1, \dots, 1)^T$, which corresponds to the mode of instability that does not affect the condition $\mathbf{x}_1 = \dots = \mathbf{x}_n$. The maximum Lyapunov exponent measuring the stability of the network-homogeneous state is then given by

$$\Lambda_{\max} := \max_{j \geq 2} \Lambda(\lambda_j), \quad (3)$$

i.e., it is stable if $\Lambda_{\max} < 0$, and unstable if $\Lambda_{\max} > 0$. In addition, $|\Lambda_{\max}|$ gives the asymptotic rate of exponential convergence or divergence.

III. OPTIMIZATION OF NETWORK STRUCTURE

We first consider the following fundamental question: *for a given number of nodes representing dynamical units, and a given number of links with identical weights, what is the assignment of links that maximize the rate of convergence to a network-homogeneous state?* We may assume A_{ij} to be binary ($A_{ij} = 0$ or 1) without loss of generality, since any link weight $\neq 1$ can be accounted for by the stability function $\Lambda(\alpha)$ (see Appendix A). We additionally assume that there is

no self-interaction, i.e., $A_{ii} = 0$. The binary-weight assumption is used in the following unless explicitly relaxed to extend our results to weighted networks.

A. Undirected networks

For the class of networks with a fixed number of undirected links $m = \sum_i \sum_{j>i} A_{ij}$, we have the additional constraint that the matrix A is symmetric. This constraint can arise from the symmetry of the physical processes underlying the interaction represented by a link, such as the diffusion of chemicals through a channel connecting reactor cells in a chemical reaction network. In this case, the optimization problem reads

$$\begin{aligned} &\text{Maximize } |\Lambda_{\max}(A)| \\ &\text{subject to } A_{ij} \in \{0, 1\}, \quad A_{ii} = 0, \quad A_{ij} = A_{ji}, \\ &\quad \sum_i \sum_{j>i} A_{ij} = m. \end{aligned} \quad (4)$$

If the stability function $\Lambda(\alpha)$ on the real line $\{\alpha \in \mathbb{C} \mid \text{Im}(\alpha) = 0\}$ is strictly decreasing for $\text{Re}(\alpha) \leq \bar{\lambda}$ (which is satisfied in most cases), maximizing the convergence rate to the network-homogeneous state for undirected networks is equivalent to maximizing λ_2 , the smallest eigenvalue excluding the null eigenvalue that exists for any networks. For $m = n(n-1)/2$, the only network with n nodes and m links is the complete graph, resulting in the (maximum) value $\lambda_2 = n$. For $m = n-1$ (implying that the network is a tree), the maximum possible value of $\lambda_2 = 1$ is achieved if and only if the network has the star configuration [46]. For other values of m (assuming $m \geq n-1$ to ensure that the network is connected), it is challenging even numerically, mainly because each A_{ij} is constrained to be either 0 or 1, which makes it a difficult non-convex combinatorial optimization. We note that the problem is also equivalent to minimizing a bound on the deviations from a network-homogeneous state in a class of networks of non-identical oscillators [51]. The maximization of λ_2 has been a subject of substantial interest in graph theory, with several notable results in the limit $n \rightarrow \infty$, assuming that each node in the network has the same degree and keeping this common degree constant [52–54] or assuming a fixed maximum degree [55]. In contrast to these sparse-network results, below we address the maximization of λ_2 in a different limit, $n \rightarrow \infty$, keeping the link density $\phi := 2m/[n(n-1)]$ constant. In the physics literature, there have been a number of studies [50, 56–60] on the related (but different) problem of maximizing the eigenratio λ_2/λ_n , which measures the synchronizability of the network structure for networks of coupled chaotic oscillators.

UCM networks—Let $0 = \lambda_1 \leq \lambda_2 \leq \dots \leq \lambda_n$ be the Laplacian eigenvalues, noting that the symmetry of A constrains them to be real. The starting point of our analysis of the λ_2 -maximization problem is the upper bound

$$\lambda_2 \leq \lfloor 2m/n \rfloor = \lfloor \phi(n-1) \rfloor, \quad (5)$$

valid for any n and m for which the link density $\phi = 2m/[n(n-1)] < 1$ (where $\lfloor x \rfloor$ denotes the largest integer

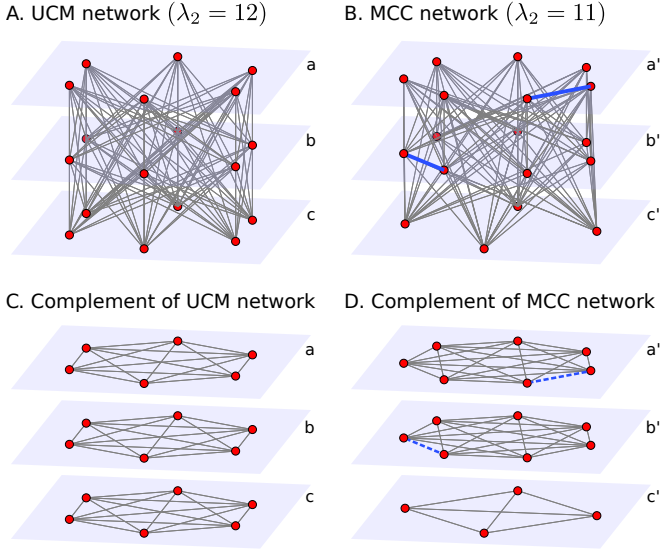


FIG. 2. UCM and MCC networks with $n = 18$ nodes. (A) The UCM network with $\ell = 3$ groups (labeled a, b, and c) of $k = 6$ nodes each. All pairs of nodes belonging to different groups are connected, while all pairs within the same group are not connected, leading to a total of $m = k^2\ell(\ell - 1)/2 = 108$ links. (B) An MCC network constructed with the same number of nodes but with one fewer link ($m = 107$) and groups of unequal sizes (labeled a', b', and c', and of sizes 7, 7, and 4, respectively). Note that in this case some nodes within the same group are connected (as indicated by solid blue lines). (C) The complement of the UCM network in panel A, which has $\ell k(k - 1)/2 = 45$ links. In the complement, a node pair is connected if they are in the same group, and not connected if they are from different groups. (D) The complement of the MCC network in panel B, which has 46 links. Since it has one more link than what can be accommodated by three isolated groups of size 6 (as in panel C), the minimum possible size of the largest component in the complement equals 7 in this case. Note that groups a' and b' have missing links (indicated by dashed blue lines), which correspond to the links within groups a' and b' in panel B. The required increase in the size of the largest component in the complement forces λ_2 to decrease by one.

not exceeding x). To prove this bound, we make use of the complement transformation, which maps a network with adjacency matrix A into the network with the adjacency matrix A^c defined by

$$A_{ij}^c = (1 - A_{ij})(1 - \delta_{ij}). \quad (6)$$

This transformation maps each nonzero eigenvalue λ_i to

$$\lambda_{n-i+2}^c = n - \lambda_i, \quad i = 2, \dots, n, \quad (7)$$

where we denote the Laplacian eigenvalues of the complement as $0 = \lambda_1^c < \lambda_2^c \leq \dots \leq \lambda_n^c$ [29, 61, 62]. The bound in Eq. (5) can then be proved by applying Proposition 3.9.3 of Ref. [63] to the complement of the network, which gives

$$\lambda_n^c \geq d_{\max}^c + 1 \geq \lceil \bar{d}^c \rceil + 1 = \lceil 2m_c/n \rceil + 1, \quad (8)$$

where d_{\max}^c and \bar{d}^c denote the maximum and mean degree of the complement, respectively. Thus, we have $\lambda_2 = n - \lambda_n^c \leq$

$n - (\lceil 2m_c/n \rceil + 1) = n - (\lceil n - 1 - 2m/n \rceil + 1) = \lfloor 2m/n \rfloor$, verifying Eq. (5).

For special combinations of n and m , namely, $n = k\ell$ and $m = k^2\ell(\ell - 1)/2$, with arbitrary positive integers ℓ and k , this bound can actually be attained by the UCM network. Here the *UCM network* is defined (for the given ℓ and k) as the network in which (i) the nodes are divided into ℓ groups of equal size k , (ii) all pairs of nodes from different groups are connected, and (iii) no pair of nodes within the same group are connected (see Fig. 2A for an example). Moreover, we can show that the UCM network is the only one that attains the bound, and thus is optimal, among all networks with the same number of nodes and links. We in fact have a more general result: for each n and m such that the mean degree $\bar{d} := 2m/n$ of the network is a nonnegative integer, λ_2 attains the upper bound $\lambda_2 = \lfloor 2m/n \rfloor$ if and only if the network is a UCM network (see Appendix B for a proof). For the cases $n = k\ell$ and $m = k^2\ell(\ell - 1)/2$, the condition on n and m is satisfied because $\bar{d} = 2m/n = k(\ell - 1) = n - k$, and our result implies that the UCM network is the only one achieving the upper bound. For other combinations of n and m for which \bar{d} is a nonnegative integer but a UCM network is not possible, the result implies that no network can achieve the upper bound.

MCC networks—For values of n and m that do not allow forming a UCM network, we consider the class of MCC networks, which we now define using a key property that makes the UCM networks optimal. To describe this property, we again make use the complement transformation. In particular, Eq. (7) implies that the maximization of λ_2 is equivalent to the minimization of λ_n^c . In terms of its complement, a UCM network consists of isolated, fully-connected clusters of equal sizes [see Fig. 2C for an example with $(\ell, k) = (3, 6)$ and Fig. 3 for examples with $(\ell, k) = (20, 1), (10, 2), (5, 4), (4, 5)$]. For a given k , let $M(n, k)$ denote the maximum number of links allowed for any n -node network whose connected components have size $\leq k$ (see Eq. (C1) in Appendix C for an explicit formula). Given m , we define $k_{n,m}$ to be the smallest (necessarily positive) integer for which $m \leq M(n, k)$; thus, $k_{n,m}$ is the minimum size of the largest connected components of any network with n nodes and m links. The key property of a UCM network we referred to above can now be expressed in terms of its complement: the size of the (largest) components equals the smallest possible value k_{n,m_c} , where $m_c := n(n - 1)/2 - m = \ell k(k - 1)/2$ is the number of links in its complement. For any network in general, the smaller the largest component size in the complement, the smaller we expect the eigenvalue λ_n^c to be, since λ_n^c is bounded by the largest component size. However, the smaller the components, the smaller the number of links they can accommodate. We thus define an MCC network as one that achieves the best possible, namely, as a network whose largest component of the complement is as small as possible among all networks with the given n and m . Formally, we call a network with n nodes and m links an *MCC network* if the largest connected component of the complement is of size k_{n,m_c} , where $m_c := n(n - 1)/2 - m$ is the number of links in the complement.

For given n and m , there can be multiple networks satisfy-

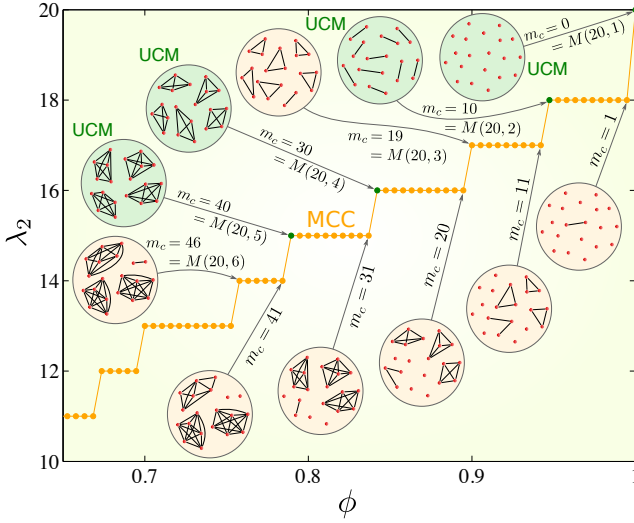


FIG. 3. UCM and MCC networks of size $n = 20$ for the maximization of smallest non-zero Laplacian eigenvalue λ_2 . For a given link density ϕ , the orange dot indicates λ_2 for MCC networks. A UCM network, when possible for that value of ϕ , is indicated by a green dot. As ϕ increases, the eigenvalue λ_2 experiences discrete jumps, corresponding to sudden changes in the structure of the network. The changes in the link configuration of the network's complement, as well as the associated jumps in the size of their largest clusters, are illustrated in the circles. At ϕ values just above and below the jumps, the complement has $m_c = M(20, k)$ links and $m_c = M(20, k) + 1$ links, respectively.

ing the above property, forming the class of MCC networks (see Fig. 2B for an example). One can explicitly construct an MCC network by forming as many isolated, fully-connected clusters of size k_{n,m_c} as possible in the complement of the network (see Appendix C). Similar strategies that suppress the size of largest connected components, when incorporated into a network growth process, have been observed to cause discontinuous, or continuous but “explosive” percolation transitions [64–67]. The deterministic growth process defined in Ref. [68] is particularly close to the definition of MCC networks in that the process explicitly minimizes the product of the sizes of the components that the new link connects in each step.

As anticipated above, the class of MCC networks inherits part of the optimality of the UCM networks: the values of λ_2 for MCC networks are locally optimal in the space of all networks with the same n and m . Indeed, we can show that the formula

$$\lambda_2 = n - k_{n,m_c} \quad (9)$$

is valid for any MCC network with link density $\phi < 1$, and that we have $\lambda_2 \leq n - k_{n,m_c}$ for any network that can be obtained from such an MCC network by rewiring a single link. We can also show that MCC networks are globally optimal in several cases of lowest and highest link densities, as well as for a range of link density around each value corresponding to a UCM network. The optimality of the networks with fully-connected clusters in the complement suggests potential sig-

nificance of other, more general network motifs [69], whose statistics has been studied in the context of network optimization [70, 71].

We can also show that, whenever an MCC network is globally (locally) optimal, it is also globally (locally) optimal when the link weights are allowed to be any positive number ≤ 1 (thus relaxing one of the assumptions we made earlier). In fact, we now prove a more general result: for any undirected networks with all link weights equal to one, the eigenvalue λ_2 of the Laplacian matrix L cannot increase as the link weights are decreased. Let L_w denote the Laplacian matrix of the network with the same set of links but with positive weights ≤ 1 . It can be shown that the matrix $L_w^c := L - L_w$ is the Laplacian matrix of another weighted network with positive link weights ≤ 1 . For each of the three (symmetric) Laplacian matrices, L , L_w , and L_w^c , denote by $\lambda_2(L)$, $\lambda_2(L_w)$, and $\lambda_2(L_w^c)$, respectively, the smallest eigenvalue excluding the identically null eigenvalue. Courant's theorem implies that $\lambda_2(L) = \min_{\mathbf{x}} \mathbf{x}^T L \mathbf{x}$, $\lambda_2(L_w) = \min_{\mathbf{x}} \mathbf{x}^T L_w \mathbf{x}$, and $\lambda_2(L_w^c) = \min_{\mathbf{x}} \mathbf{x}^T L_w^c \mathbf{x}$, where the minimum is taken over all \mathbf{x} that are perpendicular to the vector $(1, \dots, 1)^T$. Since $L = L_w + L_w^c$, it follows that

$$\begin{aligned} \lambda_2(L) &= \min_{\mathbf{x}} [\mathbf{x}^T (L_w + L_w^c) \mathbf{x}] \\ &\geq \min_{\mathbf{x}} \mathbf{x}^T L_w \mathbf{x} + \min_{\mathbf{x}} \mathbf{x}^T L_w^c \mathbf{x} \\ &= \lambda_2(L_w) + \lambda_2(L_w^c) \\ &\geq \lambda_2(L_w). \end{aligned} \quad (10)$$

Thus, $\lambda_2(L_w)$ of the network with decreased link weights cannot be larger than $\lambda_2(L)$ of the original network. Applying this result to the MCC networks, we see that these networks serve as the optimal networks within the larger class of $[0, 1]$ -weighted networks.

Sensitivity to changes in number of links or nodes—We now study the dependence of $\lambda_2 = n - k_{n,m_c}$ of an MCC network on network-structural parameters, focusing specifically on the number of nodes and links. The dependence on $\phi < 1$ through k_{n,m_c} can be expressed as

$$\lambda_2 = \lfloor C_{\ell,n}(\phi) \cdot n \rfloor, \quad (11)$$

where

$$C_{\ell,n}(\phi) = \frac{\ell^2 - \sqrt{\ell^2 - \phi \ell (\ell + 1) \left(1 - \frac{1}{n}\right)}}{\ell(\ell + 1)}, \quad (12)$$

and ℓ is the unique integer satisfying

$$1 - \frac{1}{\ell} \leq \left(1 - \frac{1}{n}\right) \phi < 1 - \frac{1}{\ell + 1}. \quad (13)$$

The value of λ_2 for MCC networks experiences a series of sudden jumps as the link density increases from $\phi = 2/n$ (the minimum possible value for a connected network, corresponding to the star configuration) to $\phi = 1$ (corresponding to the fully-connected network). This behavior is better understood by considering the complement of the network as the

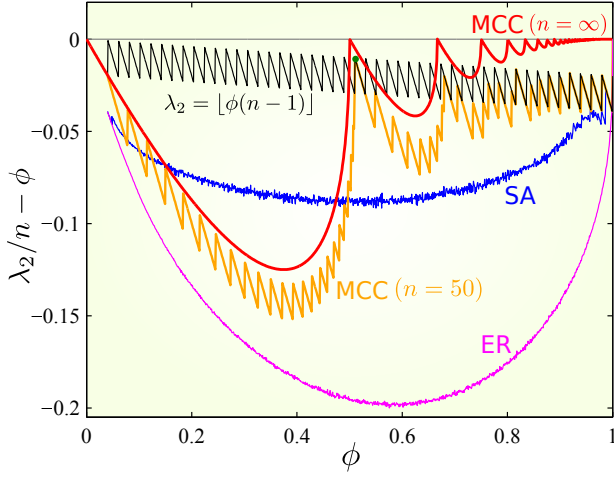


FIG. 4. Sensitive dependence of the Laplacian eigenvalue λ_2 on link density ϕ for undirected networks of size $n = 50$. Each curve indicates λ_2 normalized by the network size n , relative to the linear behavior, $\lambda_2/n = \phi$. The blue curve shows the result of a single run of SA to maximize λ_2 with a fixed number of links. The magenta curve is the average over 1,000 realizations of the ER random networks with connection probability ϕ . The orange and red curves indicate the MCC networks for $n = 50$ [Eq. (11)] and in the limit of $n \rightarrow \infty$ [Eq. (14)], respectively. Notice the square-root singularity on the left of points $\phi = \phi_\ell = \frac{\ell-1}{\ell}$, $\ell = 2, 3, \dots$, on the red curve. The green dot near one of these singularity point indicates the UCM network with $\ell = 2$ and $k = 25$, which achieves the upper bound $\lambda_2 \leq \lfloor \phi(n-1) \rfloor$ shown by the black curve.

number of links m_c in the complement increases (corresponding to decreasing link density ϕ), as illustrated for $n = 20$ in Fig. 3. When the complement has exactly $M(n, k_{n,m_c})$ links, any additional link would force the maximum component size k_{n,m_c} to increase by one, causing a jump in $\lambda_2 = n - k_{n,m_c}$. For example, when the network in Fig. 3 which has $m_c = M(20, 4) = 30$, $k_{20,30} = 4$, and $\lambda_2 = 16$ gains one more link in its complement ($m_c = 31$), the component size jumps to $k_{20,31} = 5$ and λ_2 jumps down to 15. The 18-node UCM and MCC networks in Fig. 2 also illustrate such a jump. In the context of percolation problems, similar cascades of jumps in the maximum component size, called microtransition cascades, have been identified as precursors to global phase transitions [72].

Figure 4 demonstrates that for a wide range of ϕ , the MCC networks improve λ_2 significantly over the Erdős-Rényi (ER) random networks, as well as those identified by direct numerical optimization of λ_2 using simulated annealing (SA). The difference is particularly large for ϕ near certain special values such as $1/2$. Note that the optimal value of λ_2 given by the upper bound (black curves) is achieved not only by the UCM network (for example, the one indicated by the green dot in panel B for $k = 25$, $\ell = 2$) at $\phi = 25/49 \approx 0.51$, but also by MCC networks (orange curves) for a finite range of ϕ around this value. The optimal λ_2 -value, however, is sensitive to changes in the link density ϕ , and λ_2 departs quickly from the optimal as ϕ moves away from $25/49$, particularly for $\phi < 25/49$. For larger networks, this sensitivity becomes

more prominent, and it turns into a singularity as $n \rightarrow \infty$ with fixed ϕ . To see this, we take the limit in Eq. (11) to obtain

$$\lim_{n \rightarrow \infty} \frac{\lambda_2}{n} = \frac{\ell^2 - \sqrt{\ell^2 - \phi\ell(\ell+1)}}{\ell(\ell+1)}, \quad (14)$$

where ℓ is the unique integer determined by $\phi_\ell \leq \phi < \phi_{\ell+1}$, where we define $\phi_\ell := 1 - \frac{1}{\ell} = \frac{\ell-1}{\ell}$ for any positive integer ℓ . This function of ϕ , shown in Fig. 4 (red curve), has a cusp-like dependence on ϕ around $\phi = \phi_\ell$, at which it achieves the asymptotic upper bound $\lambda_2/n \leq \phi = \lim_{n \rightarrow \infty} (\lfloor \phi(n-1) \rfloor / n)$ and has a *square-root singularity* on the left (the derivative on the left diverges, while the derivative on the right equals $1/2$). This singularity is inherently different from the discrete jumps observed above for finite n . Indeed, as the network size increases, the size of the jumps and the distance between consecutive jumps both tend to zero (as in the microtransition cascades [72] in percolation problems), making the function increasingly closer to a smooth function, while the square-root singularity becomes progressively more visible. Thus, the MCC networks asymptotically optimize λ_2 at the points where this optimized value is highly sensitive to changes in the link density.

For each singularity point $\phi = \phi_\ell$, there is a sequence of UCM networks of increasing size ($n = k\ell$, $k = 1, 2, \dots$), each of which achieves the finite- n upper bound $\lfloor \lambda_2 = (1 - \frac{1}{\ell})n \rfloor$ and whose link density $\phi = (\ell-1)/(\ell - \frac{1}{k})$ approaches ϕ_ℓ in the limit. For these networks, λ_2 scales linearly with n , and its approach to the asymptotic upper bound $\lambda_2/n \leq \phi$ is given by

$$\left| \frac{\lambda_2}{n} - \phi \right| = \frac{\phi_\ell}{n-1} = O(n^{-1}). \quad (15)$$

The networks shown in Fig. 3 for $m_c = 10, 30, 40$ are examples of such networks with $n = k\ell = 20$ and $(\ell, k) = (10, 2), (5, 4), (4, 5)$, respectively. The convergence behavior above should be compared to that of the ER networks and the networks optimized numerically by SA, for both of which we observe in our simulations the scaling

$$\left| \frac{\lambda_2}{n} - \phi \right| = O(n^{-\gamma}), \quad (16)$$

as shown in Fig. 5. For the ER networks, the results from Ref. [73] on the limiting spectral density can be used to argue that

$$\left| \frac{\lambda_2}{n} - \phi \right| \gtrsim O(n^{-1/2}), \quad (17)$$

which is consistent with the scaling observed in Fig. 5. Altogether, these scaling results indicate that the UCM networks are increasingly better in maximizing λ_2 as the network size grows, compared to networks with random links or with link configurations optimized for λ_2 numerically. More generally, for a given arbitrary ϕ the convergence of λ_2/n toward the asymptotic upper bound ϕ is much faster for the MCC networks than for the random and numerically optimized networks.

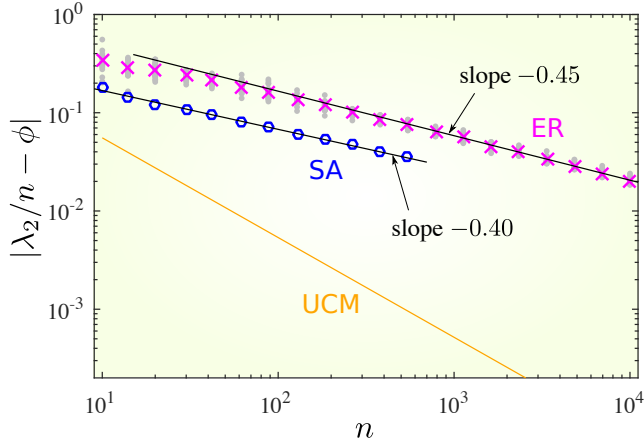


FIG. 5. Scaling behavior of λ_2 with respect to network size n . The orange line is for the UCM networks with $\ell = 2$, which have $n = 2k$ nodes and $m = k^2$ links, $k = 1, 2, \dots$, leading to the scaling behavior $|\lambda_2/n - \phi| = 1/[2(n-1)] \sim n^{-1}$. For both the ER random networks (magenta crosses) and the networks obtained by SA (blue circles), we observe the scaling $|\lambda_2/n - \phi| \sim n^{-\gamma}$ with γ significantly different from 1. For the ER random networks, we averaged over 20 realizations, which are indicated by the gray dots. Similar results are obtained for other values of ℓ .

Given that λ_2 is intimately related to the lengths of shortest paths between nodes [74, 75] (as they both reflect the connectivity of the network), it is natural to study path length statistics (and other common network statistics) of UCM and MCC networks. For UCM networks we can explicitly calculate the average length of shortest paths over all pairs of nodes. In the limit $n \rightarrow \infty$, $k \rightarrow \infty$ with ℓ fixed, the average path length approaches $2 - \phi_\ell$, which decreases linearly from two to one as the link density increases from zero to one. Thus, the UCM networks have very small path lengths. The clustering coefficient of any given node, defined as the fraction of pairs of its neighbors that are directly connected, can also be computed for the same limit and equals $2 - 1/\phi_\ell$ for $\ell \geq 2$ (for any node), which spans the entire range of possible values from zero to one as ϕ_ℓ increases from $\phi = 1/2$ ($= \phi_2$) to one.

The singular behavior seen in Fig. 4 on the left of the points $\phi = \phi_\ell$ implies that, for the MCC networks with fixed number of nodes, decreasing the link density from ϕ_ℓ can dramatically decrease λ_2 and thus the convergence rate to the network-homogeneous state. In addition to this sensitivity, λ_2 for the MCC networks has similar sensitivity with respect to another network parameter, the number of nodes n . When m is fixed, the expression for λ_2 given in Eq. (11), considered now as a function of n , has a square-root dependence on the right of the points $n = [1 + \sqrt{1 + 8m/\phi_\ell}]/2$, $\ell = 1, 2, \dots$. While increasing the number of nodes with fixed number of links in MCC networks can only decrease the convergence rate, the square-root behavior means that this drop can be very sharp.

B. Directed networks

For the class of networks with a fixed number of directed links $m_d = \sum_i \sum_{j \neq i} A_{ij}$, the matrix A can be asymmetric in general. In this case, the problem of maximizing the convergence rate can be expressed as

$$\begin{aligned} & \text{Maximize } |\Lambda_{\max}(A)| \\ & \text{subject to } A_{ij} \in \{0, 1\}, \quad A_{ii} = 0, \\ & \sum_i \sum_{j \neq i} A_{ij} = m_d. \end{aligned} \quad (18)$$

The solution of this problem generally depends on the specific shape of the stability function. If, however, the stability function is strictly decreasing in $\text{Re}(\alpha)$ and independent of $\text{Im}(\alpha)$ for $\text{Re}(\alpha) \leq \bar{\lambda} := m_d/(n-1)$, then the problem is equivalent to maximizing $\text{Re}(\lambda_2)$, the smallest real part among the eigenvalues of L excluding the identically null eigenvalue λ_1 . This is because of the upper bound $\text{Re}(\lambda_2) \leq \bar{\lambda}$, which follows from the fact that the sum of the eigenvalues equals the trace of L , which in turn equals m_d (noting that the tighter bound in Eq. (5) is not applicable to directed networks in general). If m_d is “quantized,” i.e., equals an integer multiple of $n-1$, the network can satisfy $\lambda_2 = \dots = \lambda_n = \bar{\lambda}$ [29], and hence attains the upper bound and provides a solution of the optimization problem. The class of directed networks satisfying $\lambda_2 = \dots = \lambda_n = \bar{\lambda}$ has previously been studied within the context of network synchronization using different objective functions [not defined by $\text{Re}(\lambda_2)$] compared to the convergence rate considered here [29, 33]. If m_d is not an integer multiple of $n-1$, the maximization of $\text{Re}(\lambda_2)$, like the maximization of λ_2 for undirected networks, is a hard combinatorial optimization problem.

To study the dependence of the maximum $\text{Re}(\lambda_2)$ on m_d , we compute the Laplacian eigenvalues symbolically (and thus exactly) for all directed networks of size $n = 3, 4$, and 5. For the quantized values of m_d , we verify that the upper bound $\bar{\lambda}$ is indeed attained, in which case $\lambda_2 = \dots = \lambda_n = \bar{\lambda}$ is not only real but also an integer. For intermediate values of m_d , the maximum $\text{Re}(\lambda_2)$ does not appear to follow a simple rule; it can be strictly less than $\bar{\lambda}$, have nonzero imaginary part, and/or be non-integer. In the limit of large networks, however, we can derive a simple formula; we can prove that the maximum value of $\text{Re}(\lambda_2)$, normalized by n , converges to $\phi := m_d/[n(n-1)]$ as $n \rightarrow \infty$ with fixed link density ϕ . This in particular implies that *the normalized maximum $\text{Re}(\lambda_2)$ has no sensitive dependence on ϕ* . Moreover, this result also applies to two classes of weighted directed networks: (i) networks with a fixed number of links, each with (possibly different) weight in the interval $(0, 1]$, and (ii) integer-weighted networks with a fixed sum of link weights. Thus, the networks optimizing $\text{Re}(\lambda_2)$ in these classes exhibit no sensitivity under structural perturbations in which link density is varied while keeping the network optimized. In sharp contrast to such non-generic perturbations, we see below that random (and thus generic) perturbations to the network structure can reveal sensitivity in many of these optimal networks.

IV. GENERIC PERTURBATIONS

We now study how the convergence rate behaves when a small generic perturbation is applied to the network structure, particularly when the initial network is optimal or close to being optimal. Since the convergence rate is determined by the Laplacian eigenvalues through the stability function $\Lambda(\alpha)$ and Eq. (3), it suffices to analyze how the Laplacian eigenvalues respond to generic structural perturbations, which we formulate as perturbations of the adjacency matrix in the form $A + \delta \Delta A$, where δ is a small parameter and ΔA is a fixed matrix with each ΔA_{ij} chosen randomly from a continuous distribution. This type of structural perturbations can represent imperfections in the strengths of couplings in real networks, such as power grids and networks of chemical [76], electrochemical [77], or optoelectronic [33] oscillators.

A. Directed networks

Here we show that for a given Laplacian eigenvalue λ of a directed network and a generic choice of ΔA , the change $\Delta \lambda$ of the eigenvalue due to the perturbation generally follows a scaling relation, $|\Delta \lambda| \sim \delta^\gamma$; we also provide a rigorous bound for the scaling exponent γ . This scaling exponent determines the nature of the dependence of the perturbed eigenvalue on δ : if $0 < \gamma < 1$, the dependence is sensitive and characterized by an infinite derivative at $\delta = 0$, and if $\gamma \geq 1$, it is non-sensitive and characterized by a finite derivative.

Bound on scaling exponent—We can prove the following general result on matrix perturbations, which provides an informative bound on γ . Suppose λ is an eigenvalue of an arbitrary matrix M with geometric degeneracy β [33], defined as the largest number of repetitions of λ associated with the same eigenvector (i.e., the size of the largest Jordan block associated with λ). For perturbations of the form $M + \delta \Delta M$ with an arbitrary matrix ΔM , there exists a constant C such that the corresponding change $\Delta \lambda = \Delta \lambda(\delta)$ in the eigenvalue, as a function of δ , satisfies

$$\limsup_{\delta \rightarrow 0} \frac{|\Delta \lambda(\delta)|}{\delta^{1/\beta}} \leq C. \quad (19)$$

Applying this result to an eigenvalue λ of the Laplacian matrix L , we see that $\gamma \geq 1/\beta$, implying that the set of perturbed eigenvalues that converge to λ as $\delta \rightarrow 0$ do so at a rate no slower than $\delta^{1/\beta}$.

Sensitivity to random changes in link weights—The bound established above suggests the scaling $|\Delta \lambda| \sim \delta^{1/\beta}$ for each eigenvalue of the Laplacian L . In fact, our numerics supports a more refined statement for networks under generic structural perturbations: for each eigenvector (say, the j -th one) associated with λ , there is a set of β_j perturbed eigenvalues that converge to λ as $\delta \rightarrow 0$ and follows the scaling,

$$|\Delta \lambda| \sim \delta^{1/\beta_j}, \quad (20)$$

where β_j is the number of repetitions of λ associated with the j -th eigenvector (i.e., the size of the j -th Jordan block associated with λ). We verify this individual scaling using random perturbations applied to all off-diagonal entries of A (see Fig. 6 for the results and simulation details). Since larger β_j means more sensitive dependence on δ in Eq. (20), the sensitivity of the degenerate eigenvalue λ is determined by the largest of the associated β_j 's, which is β by definition. Thus, we see that *a Laplacian eigenvalue is sensitive to generic perturbations if and only if the associated eigenvector is degenerate*, i.e., the geometric degeneracy $\beta > 1$.

To provide evidence for the tendency of network optimization to induce geometric degeneracy, we compute the Laplacian eigenvalues and the corresponding β_j symbolically (and thus exactly) for all possible directed networks of size $n \leq 5$. We find that a large fraction of the $\text{Re}(\lambda_2)$ -maximizing networks are indeed sensitive due to geometric degeneracy: 44.4%, 64.3%, and 71.5% of them have $\beta > 1$ for $n = 3, 4$, and 5, respectively. These fractions are significantly higher than the corresponding fractions among all directed networks (including non-optimal ones): 21.1%, 19.7%, and 13.7%, respectively. Since β is bounded by the algebraic degeneracy (multiplicity) of λ_2 , an interesting question is to ask how often β attains this bound, giving the network the maximum possible level of sensitivity. Among those networks that are both optimal and sensitive, 74.5% and 60.0% achieve the maximal sensitivity for $n = 4$ and 5, respectively. (The fraction is trivially 100% for $n = 3$.)

Figure 7 illustrates the range of sensitivity possible for the subclass of optimal networks satisfying $\lambda_2 = \dots = \lambda_n$, for which the maximum geometric degeneracy is $n - 1$. Non-sensitive networks in this subclass include simple cases such as the fully-connected networks and directed star networks, but also include other networks with more complicated structure, such as the network G_1 in Fig. 7. Among the sensitive networks, there is a hierarchy of networks having different levels of sensitivity, from $\beta = 2$ (e.g., network G_2 in Fig. 7) all the way up to the maximum possible value $\beta = n - 1$ (e.g., network G_{19} in Fig. 7), including all intermediate cases (e.g., network G_7 in Fig. 7).

Interestingly, the scaling behavior of the Laplacian eigenvalues also depends on the exact nature of the perturbation, and in particular the exponent can be different from $1/\beta_j$ in Eq. (20) if the perturbation is constrained to a subset of the off-diagonal entries of A . For example, when perturbing only the existing links of a directed tree (which is optimal with $\lambda_2 = \dots = \lambda_n = 1$), the exponent is one, and thus the network is not sensitive to this type of perturbations even if the degeneracy $\beta > 1$ (see Fig. 6A). This follows from the fact that the Laplacian matrix of a directed tree is triangular under appropriate indexing of its nodes, which remains true after perturbing the existing links. Such non-sensitivity to perturbations of existing links can also be shown for certain other cases, e.g., when $P^{-1} \Delta L P$ is a triangular matrix, where P is the non-singular matrix in the Jordan decomposition of L and ΔL is the perturbation of the Laplacian matrix. We note that there are also examples in which perturbing only the existing links leads to the scaling exponent $1/\beta_j$ (see Fig. 6B).

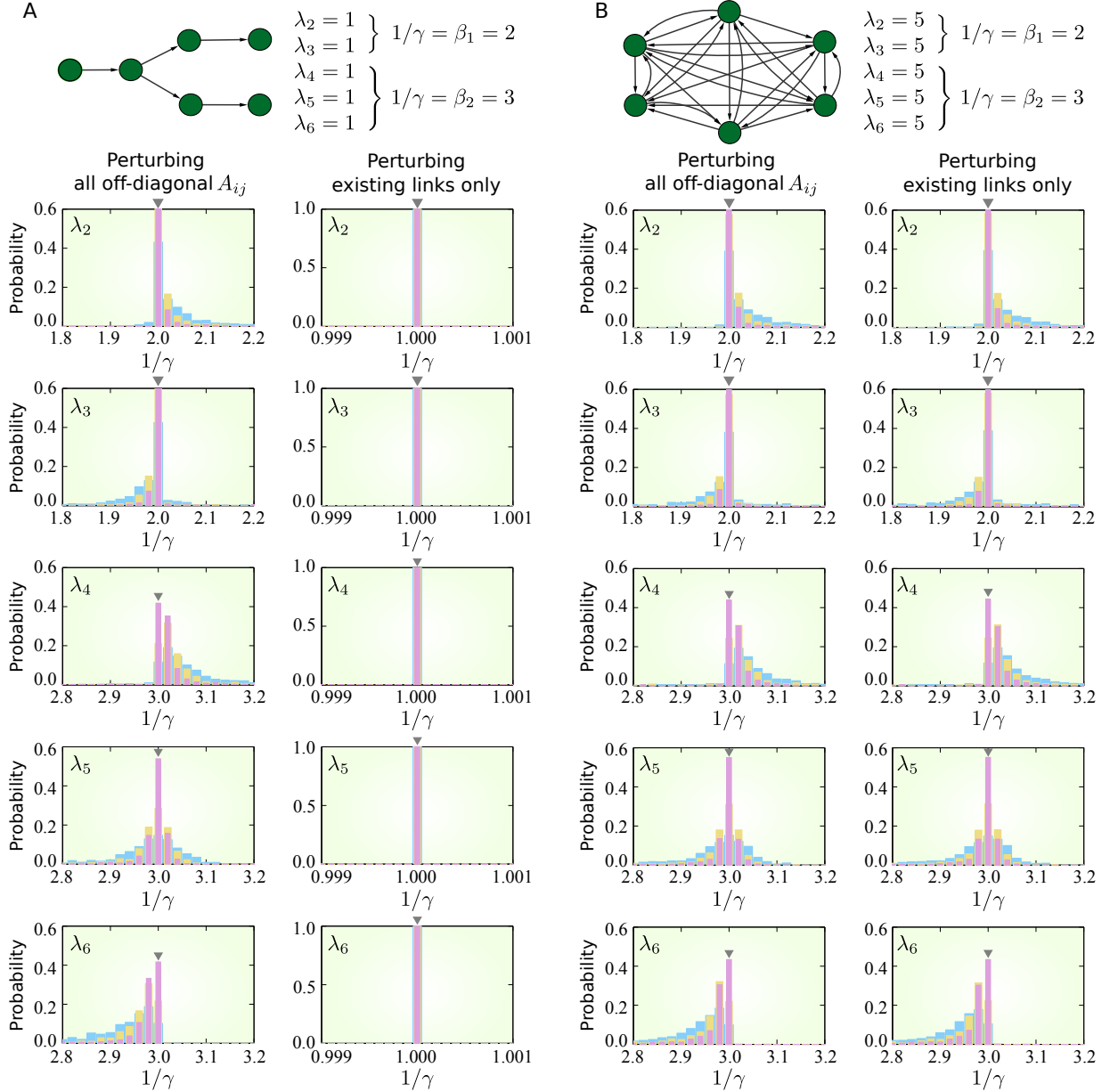


FIG. 6. Distribution of scaling exponents for Laplacian eigenvalues of 6-node optimal directed networks under random structural perturbations. (A) Example network (a directed tree) with $\lambda_2 = \dots = \lambda_6 = 1$. (B) Example network with $\lambda_2 = \dots = \lambda_6 = 5$. In each plot, the blue, yellow, and pink bars are histograms of $1/\gamma$, where γ is the scaling exponent numerically estimated using equally spaced values of δ in the intervals, $[0, 10^{-3}]$, $[0, 10^{-4}]$, and $[0, 10^{-5}]$, respectively. When perturbing all the off-diagonal entries of the adjacency matrix A (left column plots in each panel), the estimates of each exponent are distributed around β_j (indicated by the gray inverted triangles) with smaller spread for narrower ranges of δ , supporting the asymptotic scaling in Eq. (20) in the limit $\delta \rightarrow 0$. When perturbing only the existing links (right column plots in each panel), the scaling exponent depends on the initial network: the plots support $1/\gamma = 1$ for the directed tree in panel A and $1/\gamma = \beta_j$ for the network in panel B.

B. Undirected networks

For an arbitrary undirected network, for which we have the constraint that the matrix A is symmetric, *all of its Laplacian eigenvalues are non-sensitive to any (generic or non-generic) perturbation of the form $A + \delta \Delta A$* , since symmetric matrices are diagonalizable [78] and thus $\gamma \geq 1/\beta = 1$. This implies

that the rate of convergence to network-homogeneous states in any system governed by Eq. (1) with symmetric individual interactions are non-sensitive to any infinitesimal structural perturbations, independently of the optimality of the network structure. In particular, the convergence rate (as well as λ_2 itself) is non-sensitive for all UCM and MCC networks. Note that this is not in contradiction with the sensitivity of the UCM networks we discussed in Sec. III A. Indeed, consistent

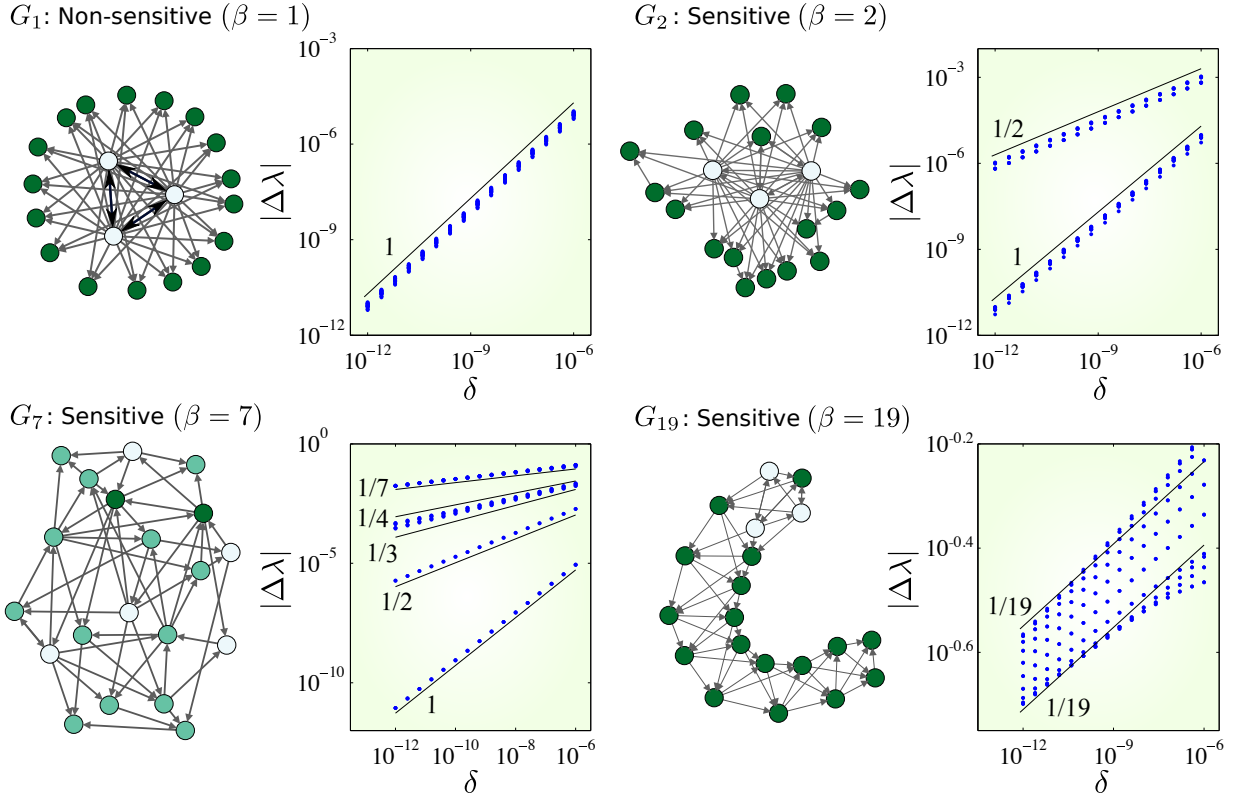


FIG. 7. Optimal directed networks with various levels of sensitivity to generic perturbations. Example networks G_1 , G_2 , G_7 , and G_{19} (each with 20 nodes and 57 links) all satisfy $\lambda_2 = \dots = \lambda_{20} = 3$ (and thus are optimal) but have different geometric degeneracy. Perturbing the adjacency matrix of each network as $A + \delta \Delta A$, we plot in double logarithmic scale the resulting change $|\Delta \lambda(\delta)| = |\lambda(\delta) - 3|$ for all 19 Laplacian eigenvalues (blue dots, many of which overlapping). The same randomly chosen ΔA is used for all four networks, where each ΔA_{ij} is drawn uniformly from the interval $[-1, 1]$ if the link exists from node j to node i , and from $[0, 1]$ otherwise. The perturbations thus allow small increase and decrease of the weight of existing links, as well as the addition of new links with small weight. In each network, nodes of the same color indicates the same in-degree, and a bidirectional arrow represents two directed links in opposite directions. The three nodes in the center of G_1 form a fully-connected triangle and each of the other nodes has three in-links from these center nodes. In each plot, we observe the expected scaling behavior in Eq. (20), indicated by black lines, each labeled with the corresponding scaling exponent, $1/\beta_j$ (G_1 : $\beta = 1$ with 19 eigenvectors and $\beta_1 = \dots = \beta_{19} = 1$; G_2 : $\beta = 2$ with 15 eigenvectors and $\beta_1 = \dots = \beta_{11} = 1$, $\beta_{12} = \dots = \beta_{15} = 2$; G_7 : $\beta = 7$ with 6 eigenvectors and $\beta_1 = \beta_2 = \beta_3 = 1$, $\beta_4 = 2$, $\beta_5 = 3$, $\beta_6 = 4$, $\beta_7 = 7$; G_{19} : $\beta = 19$ with 1 eigenvector and $\beta_1 = 19$).

with Eq. (19), we do observe that λ_2 depends linearly on δ when interpolating between any UCM network of finite size (with n nodes and m links) and any MCC network having one additional link. However, the derivative of λ_2/n as a function of link density ϕ on this interpolation interval is equal to $(n-1)/2$, which diverges as $n \rightarrow \infty$, consistent with the square-root singularity in the large-network limit established in Sec. III A. The lack of sensitivity under infinitesimal perturbations is curious since the algebraic degeneracy of λ_2 appears to be a key feature that gives these networks advantage over other undirected networks [except for some cases with $m < n(n-1)/4$] and leads to the sensitivity in the large-network limit.

C. Approximately optimal networks

Here we show that the scaling in Eqs. (19) and (20) is observed even when the eigenvector is only approximately de-

generate, which is likely the case for real-world applications where exact degeneracy is practically impossible [33]. More precisely, we show that, when the matrix is close to one with exact degeneracy, the scaling remains valid over a range of δ much larger than the distance between the two matrices. Suppose that a matrix M_0 has an eigenvalue $\lambda(M_0)$ with exact geometric degeneracy β . We consider a perturbation of M_0 in the form $M_1 = M_0 + \varepsilon \Delta M_1$, where ΔM_1 is a fixed matrix satisfying $\|\Delta M_1\| = 1$. Thus, the distance between M_0 and M_1 is ε , and for small ε (and a generic choice of ΔM_1) the matrix M_1 is approximately degenerate. We now apply a perturbation of size δ to M_1 in the form $M_2 = M_1 + \delta \Delta M_2$, where ΔM_2 is another fixed matrix satisfying $\|\Delta M_2\| = 1$. Denoting $\eta := \varepsilon/\delta$, we can write M_2 as a perturbation of M_0 rather than M_1 , namely, $M_2 = M_0 + \delta(\eta \Delta M_1 + \Delta M_2)$. When taking the limit $\delta \rightarrow 0$ with η fixed, matrices ΔM_1 and $\eta \Delta M_1 + \Delta M_2$ are both fixed, so we can apply the result in

Eq. (19). This leads to

$$\begin{aligned} \limsup_{\delta \rightarrow 0} \frac{|\lambda(M_1) - \lambda(M_0)|}{(\eta\delta)^{1/\beta}} &\leq C_1, \\ \limsup_{\delta \rightarrow 0} \frac{|\lambda(M_2) - \lambda(M_0)|}{\delta^{1/\beta}} &\leq C_2, \end{aligned} \quad (21)$$

for some constants $C_1, C_2 \geq 0$, where $\lambda(M_1)$ and $\lambda(M_2)$ denote eigenvalues of M_1 and M_2 , respectively, that approach $\lambda(M_0)$ as $\delta \rightarrow 0$. This means that for an arbitrary $\xi > 0$, we can find $\delta_1 > 0$ and $\delta_2 > 0$ (which can depend on η) such that

$$\begin{aligned} \frac{|\lambda(M_1) - \lambda(M_0)|}{(\eta\delta)^{1/\beta}} &< C_1 + \frac{\xi}{2\eta^{1/\beta}}, \quad \text{if } \delta < \delta_1, \\ \frac{|\lambda(M_2) - \lambda(M_0)|}{\delta^{1/\beta}} &< C_2 + \frac{\xi}{2}, \quad \text{if } \delta < \delta_2. \end{aligned} \quad (22)$$

Then,

$$\begin{aligned} \frac{|\lambda(M_2) - \lambda(M_1)|}{\delta^{1/\beta}} &= \frac{|[\lambda(M_2) - \lambda(M_0)] - [\lambda(M_1) - \lambda(M_0)]|}{\delta^{1/\beta}} \\ &\leq \frac{|\lambda(M_2) - \lambda(M_0)|}{\delta^{1/\beta}} + \frac{|\lambda(M_1) - \lambda(M_0)|}{(\eta\delta)^{1/\beta}} \cdot \eta^{1/\beta} \\ &< \left(C_2 + \frac{\xi}{2}\right) + \left(C_1 + \frac{\xi}{2\eta^{1/\beta}}\right) \cdot \eta^{1/\beta} \\ &= C_2 + C_1\eta^{1/\beta} + \xi, \end{aligned} \quad (23)$$

if $\delta < \min(\delta_1, \delta_2)$. Since ξ can be made arbitrarily small by making δ sufficiently small, we have

$$\limsup_{\delta \rightarrow 0} \frac{|\lambda(M_2) - \lambda(M_1)|}{\delta^{1/\beta}} \leq C_2 + C_1\eta^{1/\beta}. \quad (24)$$

Thus, Eq. (19) and the corresponding bound on the scaling exponent, $\gamma \geq 1/\beta$, remain valid for any fixed η (i.e., with $\varepsilon \rightarrow 0$ as $\delta \rightarrow 0$ while holding $\eta = \varepsilon/\delta$ constant). For finite ε and δ , this result suggests that we should observe the scaling $|\lambda(M_2) - \lambda(M_1)| \sim \delta^\gamma$ with $\gamma \geq 1/\beta$ when $\varepsilon \ll \delta \ll 1$.

Now consider the stronger scaling property in Eq. (20), which can be formalized for M_1 and M_2 as

$$\begin{aligned} \lim_{\delta \rightarrow 0} \frac{|\lambda(M_1) - \lambda(M_0)|}{(\eta\delta)^{1/\beta}} &= C_1, \\ \lim_{\delta \rightarrow 0} \frac{|\lambda(M_2) - \lambda(M_0)|}{\delta^{1/\beta}} &= C_2. \end{aligned} \quad (25)$$

Replacing Eq. (21) with Eq. (25) and using the resulting lower bounds analogous to those in Eq. (22), we obtain a lower bound analogous to that in Eq. (23). Combining this with Eq. (23), we obtain

$$\left| \frac{|\lambda(M_2) - \lambda(M_1)|}{\delta^{1/\beta}} - C_2 \right| < C_1\eta^{1/\beta} + \xi. \quad (26)$$

Since ξ can be made arbitrarily small by making δ sufficiently small, we see that $\limsup_{\delta \rightarrow 0} \left| \frac{|\lambda(M_2) - \lambda(M_1)|}{\delta^{1/\beta}} - C_2 \right| \leq$

$C_1\eta^{1/\beta}$. This implies the scaling in Eq. (20), or more precisely, $|\lambda(M_2) - \lambda(M_1)| = C\delta^{1/\beta}$ with a prefactor C that can vary with δ but is bounded between $C_2 \pm C_1\eta^{1/\beta}$ as $\delta \rightarrow 0$. The ratio η of perturbation sizes thus determines the range of variation of this scaling prefactor. In the limit of both $\eta \rightarrow 0$ and $\delta \rightarrow 0$, Eq. (26) implies $\lim_{\eta, \delta \rightarrow 0} \frac{|\lambda(M_2) - \lambda(M_1)|}{\delta^{1/\beta}} = C_2$. Therefore, we have the scaling $|\lambda(M_2) - \lambda(M_1)| \approx C_2\delta^{1/\beta}$ when $\varepsilon \ll \delta \ll 1$.

Altogether, we have shown that the scaling properties in Eqs. (19) and (20) are observed for the eigenvalues of M_2 when the size δ of the perturbation applied to M_1 is much larger compared to the distance ε between M_1 and the exactly degenerate matrix M_0 .

D. Generality of the scaling

The scaling bound in Eq. (19) is general and applies to both directed and undirected networks, both with weighted and unweighted links. We also expect the scaling in Eq. (20) to generically hold true across these classes of networks. These results are not even limited to Laplacian matrices and cover all matrices, including the adjacency matrix and any other matrix that may characterize a particular system. The degree to which the scaling holds is likely related to the normality of the Laplacian matrix, which can range from completely normal matrices with orthogonal eigenvectors (as in undirected networks), to highly non-normal matrices with parallel, degenerate eigenvectors (as in many optimal networks) [79, 80]. Combining all these with the tendency of optimization to cause geometric degeneracy and the results for approximately optimal networks in Sec. IV C (as well as the wide range of systems that Eq. (1) can describe), we expect to observe sensitivity to generic perturbations in many applications.

V. SENSITIVITY IN EXAMPLE PHYSICAL SYSTEMS

As summarized in Fig. 1, we have established two cases in which sensitive dependence on network structure arises: undirected networks under non-generic, optimized perturbations (Sec. III A) and directed networks under generic perturbations (Sec. IV A). Below we discuss implications of these cases for concrete examples of physical networked systems.

For undirected networks, the sensitivity of λ_2 observed for UCM networks is relevant for a wide range of networked systems, since the stability function formalism establishes that in many systems λ_2 determines the stability properties of relevant network-homogeneous states. Typically the asymptotic rate of convergence $|\Lambda_{\max}|$ is a smooth, monotonically increasing function of λ_2 , and thus the maximized convergence rate exhibits the cusp-like dependence on the number of nodes and links. Below we list specific cases in which sensitivity is observed in $|\Lambda_{\max}|$ or a related quantity:

1. For networks of phase oscillators, including models of power-grid networks, the convergence rate to a frequency-synchronized, phase-locked state is a function of the Lapla-

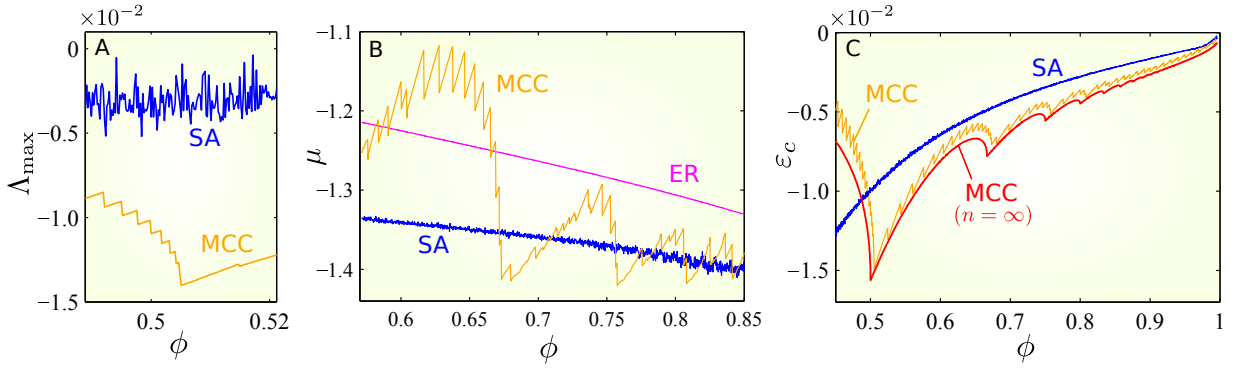


FIG. 8. Sensitive dependence on link density ϕ in physical examples of undirected networks. (A) Exponential rate of convergence Λ_{\max} to a synchronous state of power-grid networks. (B) Mean finite-time convergence rate μ toward synchronization in networks of optoelectronic oscillators. (C) Critical diffusivity threshold ε_c for Turing instability in networks of activator-inhibitor systems. The orange curves indicate the values of these quantities for the MCC networks with $n = 100$ constructed by the procedure described in Appendix C [the red curve in panel C is the finite- n approximation obtained from the asymptotic formula (14)]. The blue curves indicate the corresponding values for networks found by SA. The magenta curve in panel B is the mean value for the ER random networks estimated from 1,000 realizations. In panels A and C, the values are relative to the corresponding mean value for the ER random networks (and thus zero corresponds to the mean value).

cian eigenvalue $\tilde{\lambda}_2$ associated with the matrix \tilde{A} of effective interactions between generators. While λ_2 is generally different from $\tilde{\lambda}_2$, it is strongly correlated with λ_2 , and hence to Λ_{\max} . We thus expect to observe sensitive dependence of Λ_{\max} , which is indeed confirmed in Fig. 8A for power-grid networks with prescribed network topology and realistic parameters for the generators and other electrical components in the system.

2. In addition to the asymptotic convergence rate Λ_{\max} , sensitive dependence can be observed for the convergence rate in the transient dynamics of the network, which depends not only on λ_2 but on all Laplacian eigenvalues. This is illustrated in Fig. 8B using the example of coupled optoelectronic oscillator networks [33].
3. Another physical quantity that can exhibit sensitive dependence is the critical coupling threshold for the stability of the network-homogeneous state in systems with a global coupling strength ε . In such systems, the functions \mathbf{H}_{ij} are proportional to ε . For identical oscillators capable of chaotic synchronization, the minimum coupling strength for stable synchronization is inversely proportional to λ_2 . For the activator-inhibitor systems [45], the parameter ε is interpreted as the common diffusivity constant associated with the process of diffusion over individual links. As ε is decreased from a value sufficiently large for the uniform concentration state to be stable, there is a critical diffusivity, $\varepsilon = \varepsilon_c$, corresponding to the onset of Turing instability, and this ε_c is inversely proportional to λ_2 . Such a critical threshold thus depends sensitively on the link density of the network (as illustrated for the activator-inhibitor systems in Fig. 8C) as well as on the number of nodes.

For directed networks, the sensitivity of Laplacian eigenvalues under generic perturbations is typically inherited by the convergence rate Λ_{\max} for many systems governed by Eq. (1). In fact, Λ_{\max} would have the same sensitivity as the Laplacian eigenvalue λ_j whenever Λ_{\max} has a smooth (non-constant)

dependence on λ_j near the unperturbed values of λ_j . Figure 9 illustrates the sharp contrast between sensitive and non-sensitive cases using the example of synchronization in networks of chaotic optoelectronic oscillators [33].

VI. DISCUSSION

The sensitive dependence of collective dynamics on the network structure, characterized here by a derivative that diverges at the optimal point, has several implications. On the one hand, it implies that the dynamics can be manipulated substantially by small structural adjustments, which we suggest has the potential to lead to new control approaches based on modifying the effective structure of the network in real time; indeed, the closer the system is to being optimal, the larger the range of manipulation possible with the same amount of structural adjustment. On the other hand, the observed cusplike behavior imposes constraints on how close one can get to the ultimate optimum in practice; given an optimal network configuration at the tip of a cusp, a small parameter mismatch or deactivation/activation of nodes or links can have a significant impact on the optimality.

It is insightful to interpret our results in the context of living systems. The apparent conundrum that follows from this study is that biological networks (such as genetic, neuronal, and ecological ones) are believed to have evolved under the pressure to both optimize fitness and be robust to structural perturbations [81]. The latter means that the networks would not undergo significant loss of function (hence of optimality) when perturbed. For example, a mutation in a bacterium (i.e., a structural change to a genetic network) causes the resulting strain to be nonviable in only a minority of cases [82]. A plausible explanation is that much of the robustness of living systems comes from the plasticity they acquire from optimizing their fitness under varying conditions. In the case of bacterial organisms, for example, it is believed that the reason

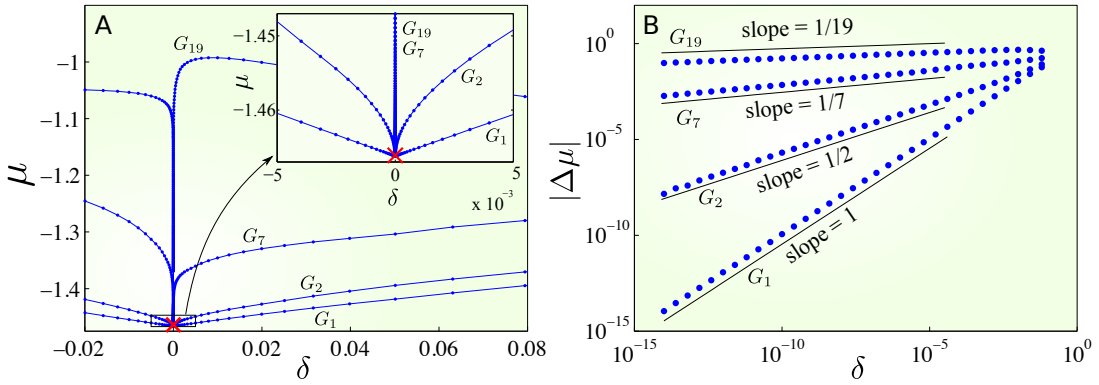


FIG. 9. Sensitivity to generic perturbations in directed networks of optoelectronic oscillators. (A) Mean convergence rate μ as a function of δ , illustrating the qualitative difference between sensitive networks (G_2 , G_7 , and G_{19} from Fig. 7) and non-sensitive networks (G_1 from Fig. 7). The red cross symbol (“ \times ”) indicates the value of μ at $\delta = 0$ corresponding to the case of no perturbation, which is the same for all four networks. (B) Log-log plot of the change in convergence rate $|\Delta\mu|$ versus δ , which confirms the scaling $|\Delta\mu| \sim \delta^{1/\beta}$ for small δ .

most of their genes are not essential for a given environmental condition is because they are required under different conditions. Bacteria kept under stable conditions, such as intracellular ones, have evolved to virtually have only those genes essential under that condition [83]; they are a close analog of optimization of a fixed objective function considered here. While there is therefore no conflict between our results and the optimization-robustness trade-off expected for biological networks, investigating the equivalent of the sensitive dependence on network structure in the case of varying conditions or varying objective function would likely provide further insights. A complementary example of interplay between optimization and robustness is described in Ref. [84], which shows that optimization can drive a population to extinction through a global bifurcation in the structure of the state space.

In general, the optimization-robustness relation may depend on the type of robustness considered. In this study we focused on how stable a state is, and hence on how resistant the network is to small changes in its dynamical state, which can be regarded as a form of robustness (terminology used, for example, in Ref. [85]). It is quite remarkable that, in seeking to optimize the network for this “dynamical” robustness it would lose “structural” robustness (i.e., how resistant the network is to changes in the network structure). But is the observed sensitive dependence on network structure really a sign of non-robustness? The answer is both yes and no. It is “yes” in the sense that, because of the non-differentiability of this dependence, small parameter changes cause stability to change significantly. It is “no” in the sense that, because the cusps appear at valleys rather than at peaks, the stability in the vicinity of the local best parameter choices are still generally better than at locations further away (that is, specific parameters lead to significant improvement but not to significant deterioration). By considering both the dynamical and structural robustness, we can interpret our results as a manifestation of the “robust-yet-fragile” property that has been suggested as a general feature of complex systems [86].

Finally, it is instructive to compare the sensitive dependence on network structure with the phenomenon of chaos, which

can exhibit multiple forms of sensitive dependence [87]. Sensitive dependence on initial conditions, where small changes in the initial state lead to large changes in the subsequent evolution of the trajectories, is a phenomenon that concerns the phase space of a fixed system. Sensitive dependence on parameters may concern a similar change in the evolution of trajectories across different systems even when the initial conditions are the same, as in the case of the map $\theta_{n+1} = 2\theta_n + c$ when c rather than θ_0 is changed. But sensitive dependence on parameters may also concern a change in the nature of the dynamics, which has a qualitative rather than just quantitative impact on the trajectories; this is the case for the logistic map $x_{n+1} = rx_n(1 - x_n)$, whose behavior can change from chaotic to periodic by arbitrarily small changes in r and, moreover, whose Lyapunov exponent exhibits a cusp-like dependence on r within each periodic window. The latter concerns sensitive dependence of the stability measure of the states under consideration, and therefore is a low-dimensional analog of the sensitive dependence of network dynamics on network structural parameters investigated here. In the case of networks, however, they emerge not from bifurcations but instead from optimization. Much in the same way the discovery of sensitive dependence on initial conditions in the context of (what is now known as) chaos set constraints on long-term predictability and on the reliability of simple models for weather forecast [88], the sensitive dependence on network structure calls for a careful evaluation of the constraints it sets on predictability and model reliability in the presence of noise and uncertainties in real network systems. We thus believe that the interplay between network structure, optimization, sensitivity, and robustness is a promising topic of future research that can offer fundamental insights into the study of complex systems.

ACKNOWLEDGMENTS

This work was supported by the U.S. National Science Foundation under Grant DMS-1057128, by the U.S.

Army Research Office under Grants W911NF-15-1-027 and W911NF-12-1-0276, and by the Simons Foundation under Grant 318812.

Appendix A: Derivation of stability function $\Lambda(\alpha)$

In Sec. II we made two assumptions on the coupling functions \mathbf{H}_{ij} , which can be formalized as follows:

- (A-1) $D_{\mathbf{u}}\mathbf{H}_{ij}(\mathbf{x}^*, \mathbf{x}^*) = -D_{\mathbf{v}}\mathbf{H}_{ij}(\mathbf{x}^*, \mathbf{x}^*)$, where $D_{\mathbf{u}}\mathbf{H}_{ij}$ and $D_{\mathbf{v}}\mathbf{H}_{ij}$ denote the derivatives with respect to the first and second argument, respectively, of the function $\mathbf{H}_{ij}(\mathbf{u}, \mathbf{v})$. We also assume $\mathbf{H}_{ij}(\mathbf{u}, \mathbf{u}) = \mathbf{0}$ for all \mathbf{u} , which ensures that the network-homogeneous state is a valid solution of Eq. (1). Together, these assumptions are equivalent to the linear approximation of \mathbf{H}_{ij} around $(\mathbf{u}, \mathbf{v}) = (\mathbf{x}^*, \mathbf{x}^*)$ given by $\mathbf{H}_{ij}(\mathbf{u}, \mathbf{v}) \approx D_{\mathbf{v}}\mathbf{H}_{ij}(\mathbf{x}^*, \mathbf{x}^*) \cdot (\mathbf{v} - \mathbf{u})$.
- (A-2) $D_{\mathbf{v}}\mathbf{H}_{ij}(\mathbf{x}^*, \mathbf{x}^*) = A_{ij} \cdot \mathbf{G}(t)$, where the scalar A_{ij} is independent of t , and the function $\mathbf{G}(t)$ is independent of i and j .

Under these assumptions, the variational equation of the system (1) around a given network-homogeneous state $\mathbf{x}_1 = \dots = \mathbf{x}_n = \mathbf{x}^*(t)$ becomes

$$\dot{\xi}_i = D_{\mathbf{x}}\mathbf{F} \cdot \xi_i - D_{\mathbf{y}}\mathbf{F} \cdot \sum_{j=1}^n L_{ij} \mathbf{G}(t) \cdot \xi_j, \quad (\text{A1})$$

where ξ_i is the perturbation to the state of unit i , $D_{\mathbf{x}}\mathbf{F}$ and $D_{\mathbf{y}}\mathbf{F}$ are the derivatives of the function \mathbf{F} with respect to the first and any of the other arguments, respectively, evaluated at $(\mathbf{x}, \mathbf{y}_1, \dots, \mathbf{y}_n) = (\mathbf{x}^*, \mathbf{0}, \dots, \mathbf{0})$, and $L = (L_{ij})$ is the Laplacian matrix of the network given by Eq. (2). An argument based on the Jordan canonical form of L similar to the one used in Ref. [57] then leads to a stability function $\Lambda(\alpha)$, defined for given (complex-valued) auxiliary parameter α as the maximum Lyapunov exponent of the solution $\boldsymbol{\eta} = \mathbf{0}$ of

$$\dot{\boldsymbol{\eta}} = [D_{\mathbf{x}}\mathbf{F} - \alpha D_{\mathbf{y}}\mathbf{F} \cdot \mathbf{G}(t)]\boldsymbol{\eta}, \quad (\text{A2})$$

which can be used to determine the stability of the network-homogeneous state. A key aspect of this approach is that the functional form of $\Lambda(\alpha)$ does not depend on the network structure, which influences the stability only through the Laplacian eigenvalues [42]. Specifically, the exponential rate of convergence or divergence is given by $\Lambda(\lambda_j)$ for the perturbation mode corresponding to the j -th (possibly complex) eigenvalue λ_j of the Laplacian matrix L . Thus, the perturbation mode with the slowest convergence (or fastest divergence) determines the stability of the network-homogeneous state through Λ_{\max} in Eq. (3).

For a system with a global coupling strength parameter ε , such as the networks of identical oscillators and networks of activator-inhibitor systems described in Secs. S1B and S1C, respectively, the derivative $D_{\mathbf{v}}\mathbf{H}_{ij}(\mathbf{x}^*, \mathbf{x}^*)$ in the condition (A-2) above is proportional to ε , and $\mathbf{G}(t)$ can be chosen to include the factor ε (thus making the stability function

$\Lambda(\alpha) = \Lambda_{\varepsilon}(\alpha)$ dependent on ε). Similarly, when considering networks with equal link weights ε for all links (as in the optimization problem described in Sec. III), ε can be factored out of A_{ij} and absorbed into $\mathbf{G}(t)$ in the condition (A-2), so that A_{ij} represents a binary network. We note that the class of systems treated in Ref. [42] is a special case of our formulation in which $\mathbf{F}(\mathbf{x}, \mathbf{y}_1, \dots, \mathbf{y}_n)$ depends linearly on the \mathbf{y} variables and the coupling function \mathbf{H}_{ij} is proportional to the difference in (some function of) the state of the nodes (see Sec. S1B). We also note that the same stability condition $\Lambda_{\max} \leq 0$ is derived in Ref. [49] for a general class of systems that is different from the class of systems treated here. This general class does not include the networks of coupled second-order phase oscillators or power generators described in Sec. S1A, since one of the assumptions on the coupling term is not satisfied. Another advantage of our formulation is that the assumptions on the nature of pairwise interactions encoded in the coupling functions \mathbf{H}_{ij} are intuitive and have clear relation to the network structure encoded in the adjacency matrix A .

Appendix B: Optimality of UCM networks

For a given undirected network with n nodes and m links, suppose that the mean degree \bar{d} is a nonnegative integer. Here we show that λ_2 attains the upper bound in Eq. (5) if and only if the network is a UCM network. Suppose first that $\lambda_2 = \lfloor 2m/n \rfloor = \bar{d}$. This implies that we have $\lambda_n^c = n - \lambda_2 = n - \bar{d}$. Also, by the assumption we made above, the mean degree of the complement, $\bar{d}^c = (n - 1) - \bar{d}$, is an integer, and thus we have $\bar{d}^c + 1 = n - \bar{d}$. Then, Eq. (8) becomes

$$n - \bar{d} = \lambda_n^c \geq d_{\max}^c + 1 \geq \bar{d}^c + 1 = n - \bar{d}. \quad (\text{B1})$$

Since this implies that the maximum and the mean degree of the complement match, i.e., $d_{\max}^c = \bar{d}^c =: d^c$, all nodes must have the same degree d^c in the complement. Now consider a connected component of the complement. On the one hand, the maximum Laplacian eigenvalue of this component is at most the maximum Laplacian eigenvalue of the entire network, $\lambda_n^c = d^c + 1$. On the other hand, it is at least $d^c + 1$ since the maximum degree of the component is d^c (by applying Proposition 3.9.3 of Ref. [63] to the component). Combining these, we conclude that the maximum Laplacian eigenvalue of this component equals $d^c + 1$. Since the maximum Laplacian eigenvalue is the maximum degree plus one, applying the second part of Proposition 3.9.3 of Ref. [63] to this component, we conclude that the size of the component is $k := d^c + 1$. Since each node in this component has degree d^c , this component must be fully connected. Note that these conclusions apply to any connected component of the complement, which implies that the number of nodes must satisfy $n = k\ell$ for some positive integer ℓ . Therefore, the complement consists of ℓ isolated fully-connected clusters of size k [and has $m_c = \ell k(k - 1)/2$ links], and the network is a UCM network. To prove the other direction of implication, suppose that the network is UCM with ℓ groups of size k . Since all components of the complement are fully connected and of size

k , the maximum Laplacian eigenvalue of the complement is $\lambda_n^c = k$. This implies that $\lambda_2 = n - k = \bar{d} = \lfloor 2m/n \rfloor$.

Appendix C: Explicit construction of MCC networks

For a given n , we first compute the function $M(n, k)$, which we recall is the maximum number of links possible for a network of size n when the largest size of connected components is $\leq k$. For each k , the maximum number of fully-connected clusters of size k that one can form with n nodes is $\ell_{n,k} := \lfloor n/k \rfloor$. Forming $\ell_{n,k}$ such clusters requires $\ell_{n,k} \cdot k(k-1)/2$ links, and completely connecting the remaining $n_r := n - k\ell_{n,k}$ nodes requires $n_r(n_r-1)/2$ links. Since any additional link would necessarily make the size of some component greater than k , this network has the maximum possible number of links, and we thus have

$$M(n, k) = \ell_{n,k} \cdot \frac{k(k-1)}{2} + \frac{n_r(n_r-1)}{2}. \quad (\text{C1})$$

Once $M(n, k)$ is computed for the given n and for each $k = 1, \dots, n$, we determine k_{n,m_c} for a given m as the

smallest integer k for which $m_c \leq M(n, k)$, where $m_c = \frac{n(n-1)}{2} - m$. The complement of an MCC network with n nodes and m links is then constructed so as to have as many fully-connected clusters of size k_{n,m_c} as possible using all the m_c available links. If one or more links remain, we recursively apply the procedure to these links and the set of remaining isolated nodes. If no cluster of size k_{n,m_c} can be formed (which occurs only when $k_{n,m_c} \geq 3$), we first construct a cluster of size $k_{n,m_c} - 1$, which is always possible since $m_c > M(n, k_{n,m_c} - 1) \geq (k_{n,m_c} - 1)(k_{n,m_c} - 2)/2$ by the definition of k_{n,m_c} . We then connect the remaining links arbitrarily while ensuring that the size of the largest connected component is k_{n,m_c} . The resulting Laplacian eigenvalues are independent of the configuration of these links, since all possible configurations are equivalent up to permutation of node indices. Note that for $n = k\ell$ and $m = k^2\ell(\ell-1)/2$, with arbitrary positive integers ℓ and k , the procedure above results in the UCM network with the number of groups $\ell_{n,k} = \ell$ and the common group size $k_{n,m_c} = k$, as it is the only MCC network in that case.

-
- [1] M. E. J. Newman, *SIAM Rev.* **45**, 167 (2003).
 - [2] S. H. Strogatz, *Nature* **410**, 268 (2001).
 - [3] A. Barrat, M. Barthélemy, and A. Vespignani, *Dynamical Processes on Complex Networks* (Cambridge University Press, 2008).
 - [4] M. A. Porter and J. P. Gleeson, *Dynamical Systems on Networks* (Springer, 2016).
 - [5] T. Nishikawa, A. E. Motter, Y. C. Lai, and F. C. Hoppensteadt, *Phys. Rev. Lett.* **91**, 014101 (2003).
 - [6] J. G. Restrepo, E. Ott, and B. R. Hunt, *Phys. Rev. E* **69**, 066215 (2004).
 - [7] H. Kori and A. S. Mikhailov, *Phys. Rev. Lett.* **93**, 254101 (2004).
 - [8] I. Belykh, V. Belykh, and M. Hasler, *Physica D* **224**, 42 (2006).
 - [9] J. G. Restrepo, E. Ott, and B. R. Hunt, *Phys. Rev. Lett.* **96**, 254103 (2006).
 - [10] D. A. Wiley, S. H. Strogatz, and M. Girvan, *Chaos* **16**, 015103 (2006).
 - [11] H. Kori and A. S. Mikhailov, *Phys. Rev. E* **74**, 066115 (2006).
 - [12] A. Arenas, A. Díaz-Guilera, J. Kurths, Y. Moreno, and C. Zhou, *Phys. Rep.* **469**, 93 (2008).
 - [13] V. Nicosia, M. Valencia, M. Chavez, A. Díaz-Guilera, and V. Latora, *Phys. Rev. Lett.* **110**, 174102 (2013).
 - [14] L. M. Pecora, F. Sorrentino, A. M. Hagerstrom, T. E. Murphy, and R. Roy, *Nat. Commun.* **5**, 4079 (2014).
 - [15] P. S. Skardal, D. Taylor, and J. Sun, *Phys. Rev. Lett.* **113**, 144101 (2014).
 - [16] V. Colizza, R. Pastor-Satorras, and A. Vespignani, *Nat. Phys.* **3**, 276 (2007).
 - [17] S. Gómez, A. Díaz-Guilera, J. Gómez-Gardeñes, C. J. Pérez-Vicente, Y. Moreno, and A. Arenas, *Phys. Rev. Lett.* **110**, 028701 (2013).
 - [18] F. Sorrentino, M. di Bernardo, F. Garofalo, and G. Chen, *Phys. Rev. E* **75**, 046103 (2007).
 - [19] S. Sreenivasan, R. Cohen, E. López, Z. Toroczkai, and H. E. Stanley, *Phys. Rev. E* **75**, 036105 (2007).
 - [20] A. Pomerance, E. Ott, M. Girvan, and W. Losert, *Proc. Nat. Acad. Sci. USA* **106**, 8209 (2009).
 - [21] L. A. Bunimovich and B. Z. Webb, *Nonlinearity* **25**, 211 (2012).
 - [22] S. Hata, H. Nakao, and A. S. Mikhailov, *Phys. Rev. E* **89**, 020801 (2014).
 - [23] J. Sun, D. Taylor, and E. M. Bollt, *SIAM J. Appl. Dyn. Syst.* **14**, 73 (2015).
 - [24] C. Fu, Z. Deng, L. Huang, and X. Wang, *Phys. Rev. E* **87**, 032909 (2013).
 - [25] Y. Qian, X. Huang, G. Hu, and X. Liao, *Phys. Rev. E* **81**, 036101 (2010).
 - [26] T. Gross, C. J. D. D'Lima, and B. Blasius, *Phys. Rev. Lett.* **96**, 208701 (2006).
 - [27] S. Risau-Gusman and D. H. Zanette, *J. Theor. Biol.* **257**, 52 (2009).
 - [28] A. Hagberg and D. A. Schult, *Chaos* **18**, 037105 (2008).
 - [29] T. Nishikawa and A. E. Motter, *Proc. Nat. Acad. Sci. USA* **107**, 10342 (2010).
 - [30] T. Watanabe and N. Masuda, *Phys. Rev. E* **82**, 046102 (2010).
 - [31] J. D. Hart, J. P. Pade, T. Pereira, T. E. Murphy, and R. Roy, *Phys. Rev. E* **92**, 022804 (2015).
 - [32] N. A. M. Araújo, H. Seybold, R. M. Baram, H. J. Herrmann, and J. S. Andrade, *Phys. Rev. Lett.* **110**, 064106 (2013).
 - [33] B. Ravoori, A. B. Cohen, J. Sun, A. E. Motter, T. E. Murphy, and R. Roy, *Phys. Rev. Lett.* **107**, 034102 (2011).
 - [34] M. Nixon et al., *Phys. Rev. Lett.* **108**, 214101 (2012).
 - [35] I. Dobson, B. A. Carreras, V. E. Lynch, and D. E. Newman, *Chaos* **17**, 026103 (2007).
 - [36] D. L. K. Yamins et al., *Proc. Nat. Acad. Sci. USA* **111**, 8619 (2014).
 - [37] G. Buzsáki, C. Geisler, D. A. Henze, and X. J. Wang, *Trends Neurosci.* **27**, 186 (2004).

- [38] G. Tononi, O. Sporns, and G. M. Edelman, *Proc. Nat. Acad. Sci. USA* **91**, 5033 (1994).
- [39] E. Bullmore and O. Sporns, *Nat. Rev. Neurosci.* **10**, 186 (2009).
- [40] S. Achard and E. Bullmore, *PLoS Comput. Biol.* **3**, e17 (2007).
- [41] B. D. MacArthur and R. J. Sánchez-García, *Phys. Rev. E* **80**, 026117 (2009).
- [42] L. M. Pecora and T. L. Carroll, *Phys. Rev. Lett.* **80**, 2109 (1998).
- [43] W. Ren, R. Beard, and E. Atkins, *IEEE Control Syst. Magazine* **27**, 71 (2007).
- [44] P. Yang, R. Freeman, and K. Lynch, *IEEE T. Automat. Contr.* **53**, 2480 (2008).
- [45] H. Nakao and A. S. Mikhailov, *Nat. Phys.* **6**, 544 (2010).
- [46] C. Maas, *Discrete Appl. Math.* **16**, 31 (1987).
- [47] A. E. Motter, S. A. Myers, M. Anghel, and T. Nishikawa, *Nat. Phys.* **9**, 191 (2013).
- [48] Y. Kuramoto, *Chemical Oscillations, Waves, and Turbulence* (Springer-Verlag, 1984).
- [49] K. S. Fink, G. Johnson, T. Carroll, D. Mar, and L. Pecora, *Phys. Rev. E* **61**, 5080 (2000).
- [50] T. Nishikawa and A. E. Motter, *Phys. Rev. E* **73**, 065106 (2006).
- [51] J. Sun, E. M. Bollt, and T. Nishikawa, *Europhys. Lett.* **85**, 60011 (2009).
- [52] N. Alon, *Combinatorica* **6**, 83 (1986).
- [53] A. Lubotzky, R. Phillips, and P. Sarnak, *Combinatorica* **8**, 261 (1988).
- [54] J. Friedman, J. Kahn, and E. Szemerédi, *STOC '89 Proceedings of the twenty-first annual ACM symposium on Theory of computing*, New York, NY, USA, 587 (1989).
- [55] T. Kolokolnikov, *Linear Algebra Appl.* **471**, 122 (2015).
- [56] L. Donetti, P. I. Hurtado, and M. A. Muñoz, *Phys. Rev. Lett.* **95**, 188701 (2005).
- [57] T. Nishikawa and A. E. Motter, *Physica D* **224**, 77 (2006).
- [58] B. Wang, T. Zhou, Z. L. Xiu, and B. J. Kim, *Eur. Phys. J. B* **60**, 89 (2007).
- [59] M. Brede, *Phys. Rev. E* **81**, 025202 (2010).
- [60] Q. Xinyun, W. Lifu, G. Yuan, and W. Yaping, *The optimal synchronizability of a class network, 25th Chinese Control and Decision Conference*, 3414 (2013).
- [61] R. Diestel, *Graph Theory* (Springer-Verlag, 2005).
- [62] Z. Duan, C. Liu, and G. Chen, *Physica D* **237**, 1006 (2008).
- [63] A. Brouwer, *Spectra of Graphs* (Springer, 2012).
- [64] D. Achlioptas, R. M. D'Souza, and J. Spencer, *Science* **323**, 1453 (2009).
- [65] R. A. da Costa, S. N. Dorogovtsev, A. V. Goltsev, and J. F. F. Mendes, *Phys. Rev. Lett.* **105**, 255701 (2010).
- [66] O. Riordan and L. Warnke, *Science* **333**, 322 (2011).
- [67] R. M. D'Souza and J. Nagler, *Nat. Phys.* **11**, 531 (2015).
- [68] H. Rozenfeld, L. Gallos, and H. Makse, *Eur. Phys. J. B* **75**, 305 (2010).
- [69] R. Milo, S. Shen-Orr, S. Itzkovitz, N. Kashtan, D. Chklovskii, and U. Alon, *Science* **298**, 824 (2002).
- [70] O. Sporns and R. Kötter, *PLoS Biol.* **2**, e369 (2004).
- [71] P. Kaluza, M. Ipsen, M. Vingron, and A. S. Mikhailov, *Phys. Rev. E* **75**, 015101 (2007).
- [72] W. Chen, M. Schröder, R. M. D'Souza, D. Sornette, and J. Nagler, *Phys. Rev. Lett.* **112**, 155701 (2014).
- [73] M. Bauer and O. Golinelli, *J. Stat. Phys.* **103**, 301 (2001).
- [74] B. Mohar, *Graph. Combinator.* **7**, 53 (1991).
- [75] A. A. Rad, M. Jalili, and M. Hasler, *Linear Algebra Appl.* **435**, 186 (2011).
- [76] A. F. Taylor, M. R. Tinsley, and K. Showalter, *Phys. Chem. Chem. Phys.* **17**, 20047 (2015).
- [77] I. Z. Kiss, Y. Zhai, and J. L. Hudson, *Science* **296**, 1676 (2002).
- [78] G. Golub and C. Van Loan, *Matrix Computations* (Johns Hopkins University Press, 2013).
- [79] L. Trefethen and M. Embree, *Spectra and Pseudospectra: The Behavior of Nonnormal Matrices and Operators* (Princeton University Press, 2005).
- [80] A. Milanese, J. Sun, and T. Nishikawa, *Phys. Rev. E* **81**, 046112 (2010).
- [81] H. Kitano, *Nat. Rev. Genet.* **5**, 826 (2004).
- [82] T. Baba et al., *Mol. Syst. Biol.* **2**, 2006.0008 (2006).
- [83] J. I. Glass, et al., *Proc. Nat. Acad. Sci. USA* **103**, 425 (2006).
- [84] K. Parvinen and U. Dieckmann, *J. Theor. Biol.* **333**, 1 (2013).
- [85] Y. Bar-Yam and I. R. Epstein, *Proc. Nat. Acad. Sci. USA* **101**, 4341 (2004).
- [86] J. M. Carlson and J. Doyle, *Phys. Rev. E* **60**, 1412 (1999).
- [87] E. Ott, *Chaos in Dynamical Systems*, 2nd ed. (Cambridge University Press, 2002).
- [88] E. N. Lorenz, *J. Atmos. Sci.* **20**, 130 (1963).